ELASTIC INITIAL AND POST-LOCAL BUCKLING OF PROFILED TROUGH GIRDERS

M. Azhari

Department of Civil Engineering
Isfahan University of Technology
Isfahan, Iran

M. A. Bradford

The University of New South Wales
Australia

Abstract An experiment investigating the elastic local buckling response of trough girders composed of thin profiled steel sheeting has been undertaken. Beam tests were performed to promote initial local buckling in a region of constant moment in the elastic range of structural response. The results of the experiments were compared with an elastic complex semi-analytical finite strip method of analysis, and acceptable correlation was obtained. The post-local buckling behavior was monitored in the experiments, and this response showed good agreement with a nonlinear finite strip method developed elsewhere.

Key Words Cold Formed, Finite Strip, Girders, Local Buckling, Postbuckling, Profiled, Sheeting

چکیده آزمایشهایی برای تحقیق در مورد کمانش ارتجاعی تیرهای متشکل از صفحات فلزی نازک انجام پذیرفته است. تیرهائی به منظور ظهور پدیده کمانش اولیه در ناحیه لنگر خمشی ثابت و در محدوده واکنش ارتجاعی مورد آزمایش قرار گرفتند. نتایج تجربی با نتایج تحلیلی که از روش نوارهای محدود مختلط بدست آمده مورد مقایسه قرار گرفته و انطباق خوبی حاصل گردیده است. رفتار بعد از کمانش نیز بصورت تجربی مورد مشاهده قرار گرفته و نتایج حاصله موافقت خوبی با نتایج تحلیلی که از روش نوارهای محدود غیرخطی بدست می آید را نشان می دهد.

INTRODUCTION

Cold formed profiled steel sheeting has been used for profiled composite slab construction for a number of years, and it results in a saving in construction time, labour and materials [1]. The advantages with accrue to composite slabs have been applied to profiled composite walls [2] and profiled composite beams [3], [4] and [5].

Profiled composite beams are a new form of construction formed by assembling a series of profiled steel sheets together either by pre-fabrication or on site. The former method results in a profiled trough girder which contains internal bracing and is designed to withstand the forces to which it is subjected during construction, particularly wet concrete loading. The behavior of profiled trough girders before wet concrete loading will involve in-plane stresses, which when large enough, can cause local instability in zone of high compressive stresses [6].

This paper presents the results of an analytical and experimental study of empty profiled trough griders tested in bending to ascertain the elastic local buckling behavior. Two profiled trough girders were subjected to a two-point loading arrangement to simulated uniform bending. The deformations of the cross-section, which included the load-deflection characteristics for the in-plane and out-of-plane deformations, were monitord. The longitudinal strains were also monitored in the compression zone on both

sides of the beams beyond the onset of the initial local buckling. The beams were designed to buckle locally in the constant moment region in the elastic range of structural response.

A theoretical model based on a very efficient complex finite strip method incorporating the so-called bubble functions developed by Azhari and Bradford [7] was used to validate the initial local buckling stresses. Post-local buckling was then studied theoretically using a nonlinear finite strip model developed by Azhari and Bradford [8] which incorporates the use of bubble functions. This postbuckling response was compared with that of obtained from the tests.

THEORY

The theoretical model deployed for comparison with the experiments was the semi-analytical initial finite strip method developed by Azhari and Bradford [7], and the finite strip postbuckling analysis developed by Azhari and Bradford [8]. This latter postbuckling analysis differs from other treatments in its use of so-called bubble functions, which are extra modes, zero on the boundaries, representing additional strip degrees of freedom. The main advantages of the bubble-strip formulation are in the reduction of the number of strips into which the topology is divided, and in substantially more rapid convergence of the nonlinear stiffness equations.

These advantages are germane to the present study, since the profiled topology is complex and the number of nonlinear simultaneous equations is correspondingly large. Bradford and Hancock [9] first formulated a post-local buckling analysis using the finite strip method which employed two longitudinal harmonics. The flexural displacements were modified by Azhari and Bradford [8] to include a quartic bubble, so that the flexural deformation w of the strip in Figure 1 can be written as

$$w = (\alpha_1 + \alpha_2\eta + \alpha_3\eta^2 + \alpha_4\eta^3 + \alpha_5\eta^4)\sin\xi \quad (1)$$

and

$$w_0 = (\alpha_{10} + \alpha_{20}\eta + \alpha_{30}\eta^2 + \alpha_{40}\eta^3 + \alpha_{50}\eta^4)\sin\xi \quad (2)$$

where w_0 is the initial sinusoidal geometric imperfection, $\alpha_1,\ldots,\alpha_5$ are polynomial coefficients, $\alpha_{10}, \ldots,\alpha_{50}$ are coefficients determined prior to the analysis, and where

$$\xi = \frac{\pi x}{\lambda} \quad (3)$$

and

$\eta = \frac{y}{\lambda}$ buckling half-wavelength.

The vector of flexural strains in the strip $\{\Delta\varepsilon_f\} = \varepsilon_f - \varepsilon_{f0}$ is written from usual linear theory as

$$\{\Delta\varepsilon_f\} = \begin{Bmatrix} \frac{\partial^2 (w - w_0)}{\partial x^2} \\ \frac{\partial^2 (w - w_0)}{\partial y^2} \\ \frac{2\,\partial^2 (w - w_0)}{\partial x \partial y} \end{Bmatrix} \quad (5)$$

while for the membrane strains $\{\Delta\varepsilon_m\}$, use must be made of nonlinear theory if the response in the post-

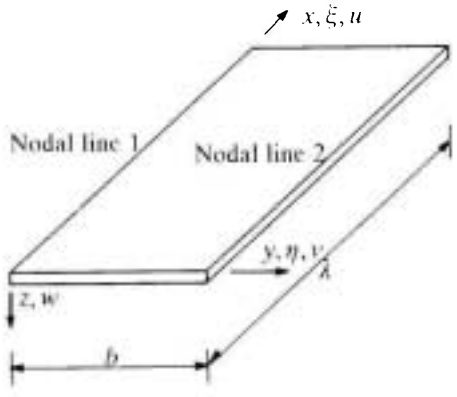

Figure 1. Finite strip.

locally buckled domain is to be obtained. Hence the membrane strains are

$$\{\Delta\varepsilon_m\} = \begin{Bmatrix} \frac{\partial(u-u_0)}{\partial x} + \frac{1}{2}\left[\left(\frac{\partial w}{\partial x}\right)^2 - \left(\frac{\partial w_0}{\partial x}\right)^2\right] \\ \frac{\partial v}{\partial y} + \frac{1}{2}\left[\left(\frac{\partial w}{\partial y}\right)^2 - \left(\frac{\partial w_0}{\partial y}\right)^2\right] \\ \frac{\partial(u-u_0)}{\partial y} + \frac{\partial v}{\partial x} + \left(\frac{\partial w}{\partial x}\right)\left(\frac{\partial w}{\partial y}\right) - \left(\frac{\partial w_0}{\partial x}\right)\left(\frac{\partial w_0}{\partial y}\right) \end{Bmatrix} \quad (5)$$

in which u_0 is the initial in-plane displacement. Since the initial in-plane imperfection is much less than the initial out-of-plane imperfection, u_0 can be assumed to be negligible.

The elastic isotripic plate property matrix $[D]$ defines the membrane and flexural stress-strain relationship by

$$\{\Delta\sigma\} = [D]\ \{\Delta\varepsilon\} \quad (7)$$

The vector $\{\Delta\sigma\}$ contains the incremental resultant bending moments and torsional moments and the resultant forces per unit length of plate, membrane normal and shear stresses.
where

$$[D] = \begin{bmatrix} [D_f] & . \\ . & [D_m] \end{bmatrix} \quad (8)$$

$$[D_m] = \frac{E}{1-\nu^2}\begin{bmatrix} 1 & \nu & 0 \\ \nu & 1 & 0 \\ 0 & 0 & \frac{1-\nu}{2} \end{bmatrix} \quad (9)$$

$$[D_f] = \frac{t^3}{12}[D_m] \quad (10)$$

The remainder of the finite strip formulation follows routine elastic stiffness procedures, coupled with the principle of virtual displacements, as is fully set-out by Azhari and Bradford [8]. When this is done, the total structural nonlinear stiffness equations can be written as

$$\left([K] + [S] + [K_1(\Delta)] + \frac{1}{2}[K_1(\Delta)]^T + [K_2(\Delta^2)] - [K_2(\Delta_0^2)]\right)\{\Delta\} = \left([K] + \frac{1}{2}[K_1(\Delta_0)]^T\right)\{\Delta_0\} - \{F\} \quad (11)$$

where:
$\{\Delta\}$ = the global displacement vector;
$[K]$ = the constant linear component of the stiffness matrix;
$[S]$ = the stability matrix which is a function of the longitudinal applied stresses;
$[K_1(\Delta)]$ = the nonliner component of the stiffness matrix which is a linear function of the nodal line displacements;
$[K_1(\Delta^2)]$ = the nonlinear component of the stiffness matrix which is a quadratic function of the nodal line displacements;
$\{F\}$ = the load vector resulting from the longitudinal compressive strains; and
$\{\Delta_0\}$ = the vector of initial values of the nodal line displacements.

Equation 11 is nonlinear and not symmetric, and recourse must be made to a numerical scheme for its solution. For this, the Newton-Raphson method as presented by Gallager [10] for nonlinear finite element problem was used.

Following this method, the tangent stiffness relationship which relates the incremental loads $\{dF\}$ to the incremental displacement $\{d\Delta\}$ may be written as follows:

$$\{dF\} = [T]\ \{d\Delta\} \quad (12)$$

Azhari and Bradford [8] determined the tangent

stiffness matrix $[T]$ by formal tensor differentiation in their derivation, and showed that it could be expressed by the symmetric matrix

$$[T] = [K] + [S] + [K_1(\Delta)] + [K_1(\Delta)]^T + 2\,[K_2(\Delta^2)] + [H_1(\Delta)] - [H_1(\Delta_0)] + [H_2(\Delta^2)] - \left[H_2(\Delta_0^2)\right] \quad (13)$$

In order to use Equation 11 for initial local buckling, it may be linearised by setting $\{F\} = \{0\}$, $\{\Delta_0\} = \{0\}$ and neglecting the nonlinear stiffness matrix, producing the well-known expression

$$([K]) + [S])\ \{\Delta\} = \{0\} \quad (14)$$

For nontrival $\{\Delta\}$, Equation 14 represents a standard eigenproblem which may be solved for the critical strain distribution (the eigenvalue) and the buckled shape $\{\Delta\}$ (the eigenvector). Note that the eigenvector $\{\Delta\}$ in Equation 14 was used as the basis for determining the vector of geometric imperfections $\{\Delta_0\}$ for use in the nonlinear theory.

EXPERIMENTS

Two profiled trough girders denoted (B1 and B2) were tested in a constant moment region to promote the onset of elastic local buckling. The loading was then continued past the initial local buckling load. The cross-sections of the trough girders are shown in Figure 2 and the set-up used for the experiments is illustrated in Figure 3. Of the two beams B1 had a **b/t** ratio of 100 while B2 had a **b/t** ratio 80. The transverse deflections were measured using linear varying displacement transducers (LVDT) in the constant moment region. Lateral deflections were obtaiend using LVDT's mounted on each side of the beam at various depths throughout the cross-sections. Strains were measured in the top flange and top rip of the beams on either side. The constant moment region used for the test was of 1 meter length.

EXPERIMENTAL RESULTS

Transverse Load-deflection Plots

The transverse load-deflection response was monitored on opposite sides of the beam, in order to obtain any rotation that might have occurred through eccentric loading. The load deflection reponse of beams B1 and B2 are shown in Figures 4 and 5 respectively. It can be seen that, as expected, the

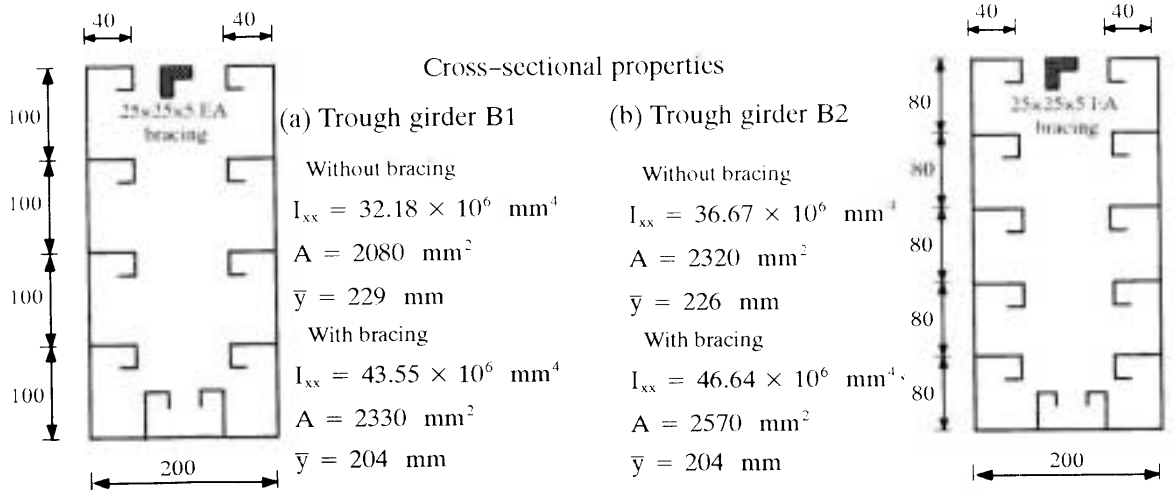

Figure 2. Trough girder cross-sections.

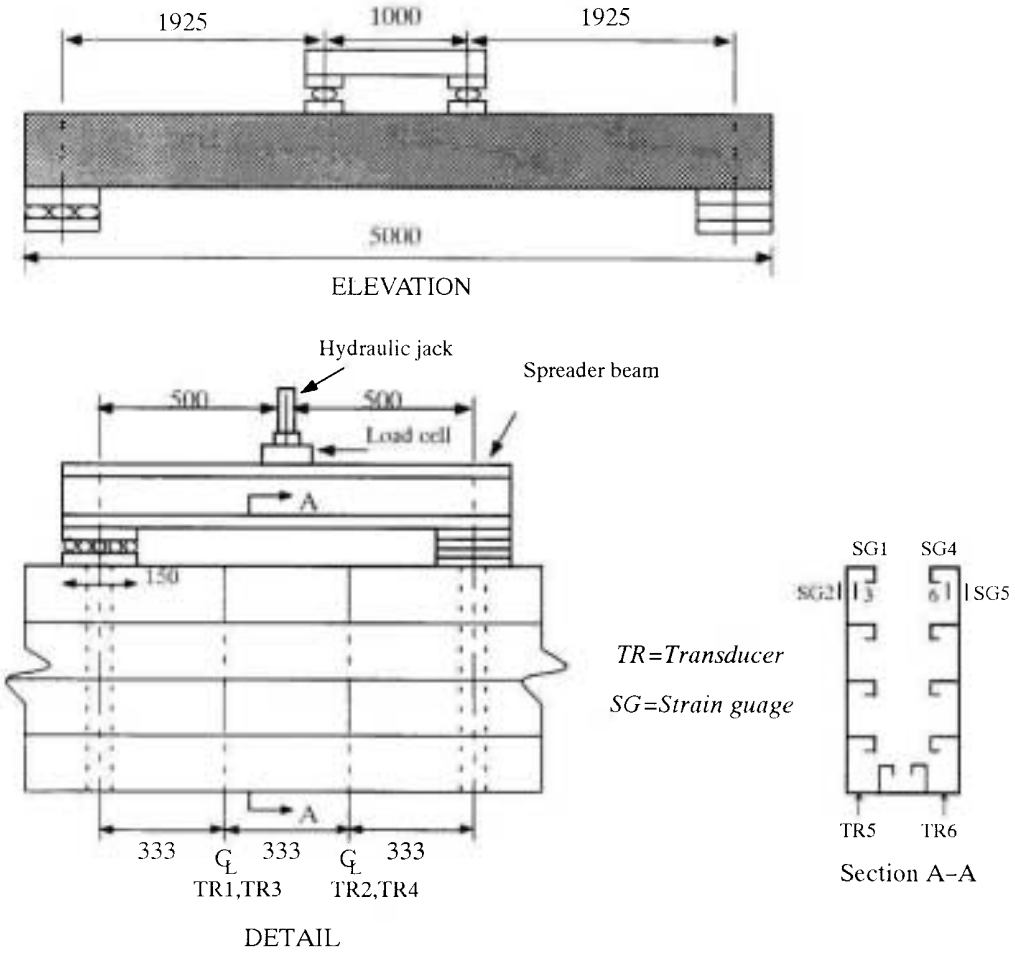

Figure 3. Experimental test set-up of trough girders.

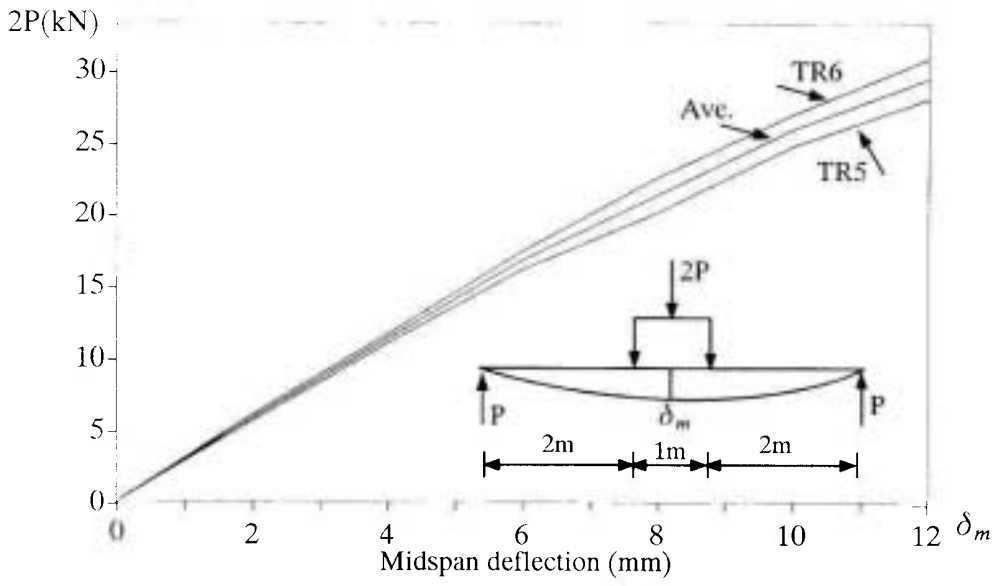

Figure 4. Load-deflection of profiled trough girder B1.

stiffness matrix $[T]$ by formal tensor differentiation in their derivation, and showed that it could be expressed by the symmetric matrix

$$[T] = [K] + [S] + [K_1(\Delta)] + [K_1(\Delta)]^T + 2\,[K_2(\Delta^2)] + [H_1(\Delta)] - [H_1(\Delta_0)] + [H_2(\Delta^2)] - \left[H_2(\Delta_0^2)\right] \quad (13)$$

In order to use Equation 11 for initial local buckling, it may be linearised by setting $\{F\} = \{0\}$, $\{\Delta_0\} = \{0\}$ and neglecting the nonlinear stiffness matrix, producing the well-known expression

$$([K]) + [S])\ \{\Delta\} = \{0\} \quad (14)$$

For nontrival $\{\Delta\}$, Equation 14 represents a standard eigenproblem which may be solved for the critical strain distribution (the eigenvalue) and the buckled shape $\{\Delta\}$ (the eigenvector). Note that the eigenvector $\{\Delta\}$ in Equation 14 was used as the basis for determining the vector of geometric imperfections $\{\Delta_0\}$ for use in the nonlinear theory.

EXPERIMENTS

Two profiled trough girders denoted (B1 and B2) were tested in a constant moment region to promote the onset of elastic local buckling. The loading was then continued past the initial local buckling load. The cross-sections of the trough girders are shown in Figure 2 and the set-up used for the experiments is illustrated in Figure 3. Of the two beams B1 had a **b/t** ratio of 100 while B2 had a **b/t** ratio 80. The transverse deflections were measured using linear varying displacement transducers (LVDT) in the constant moment region. Lateral deflections were obtaiend using LVDT's mounted on each side of the beam at various depths throughout the cross-sections. Strains were measured in the top flange and top rip of the beams on either side. The constant moment region used for the test was of 1 meter length.

EXPERIMENTAL RESULTS

Transverse Load-deflection Plots

The transverse load-deflection response was monitored on opposite sides of the beam, in order to obtain any rotation that might have occurred through eccentric loading. The load deflection reponse of beams B1 and B2 are shown in Figures 4 and 5 respectively. It can be seen that, as expected, the

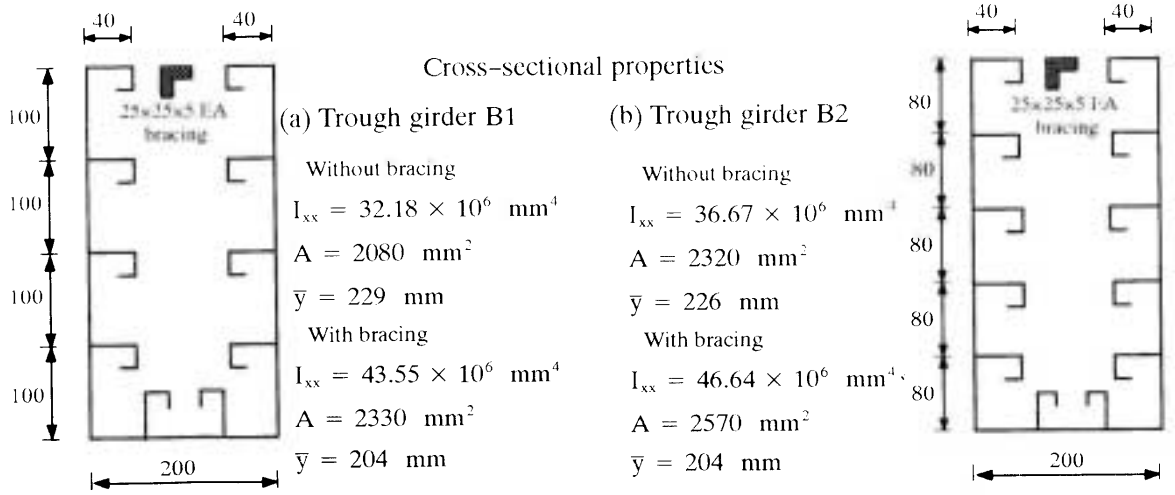

Figure 2. Trough girder cross-sections.

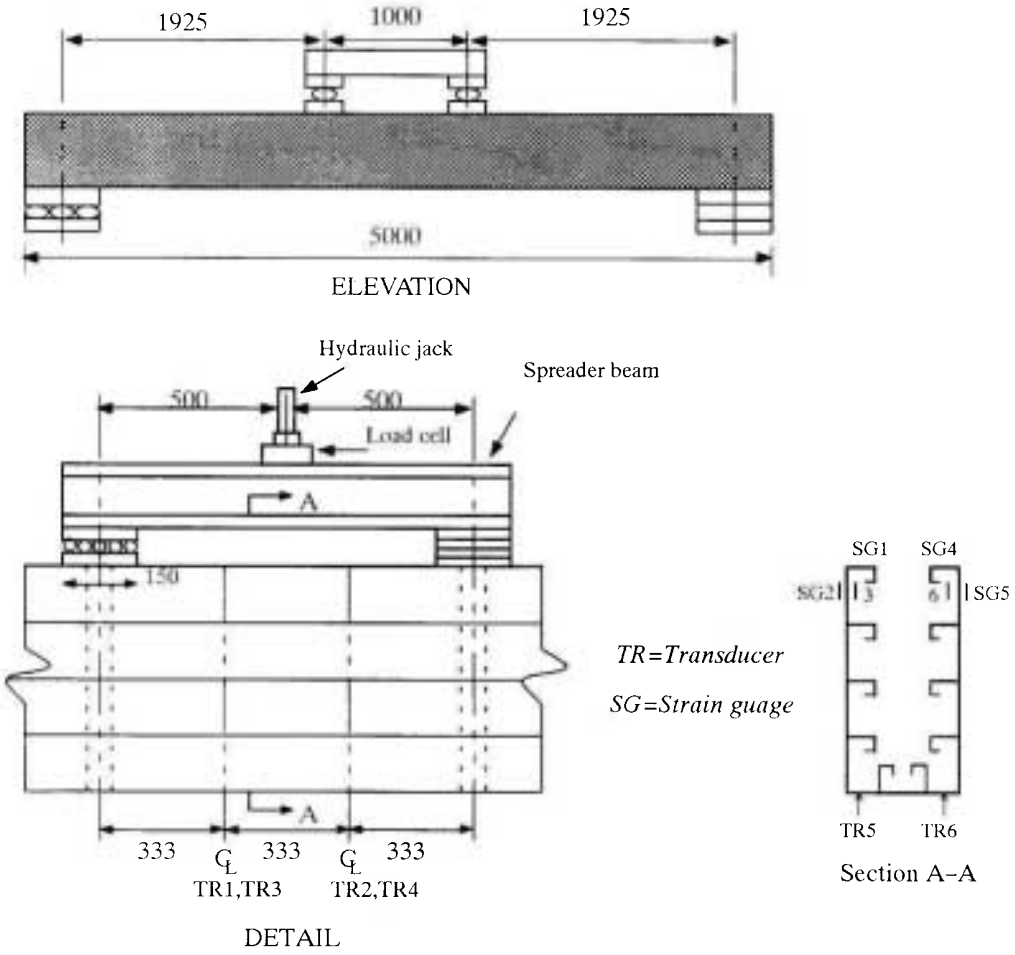

Figure 3. Experimental test set-up of trough girders.

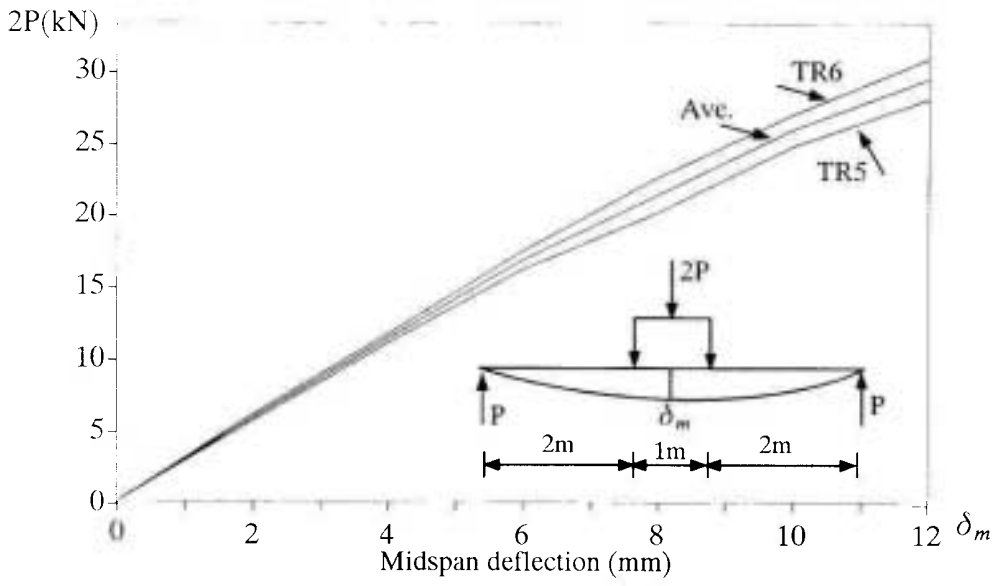

Figure 4. Load-deflection of profiled trough girder B1.

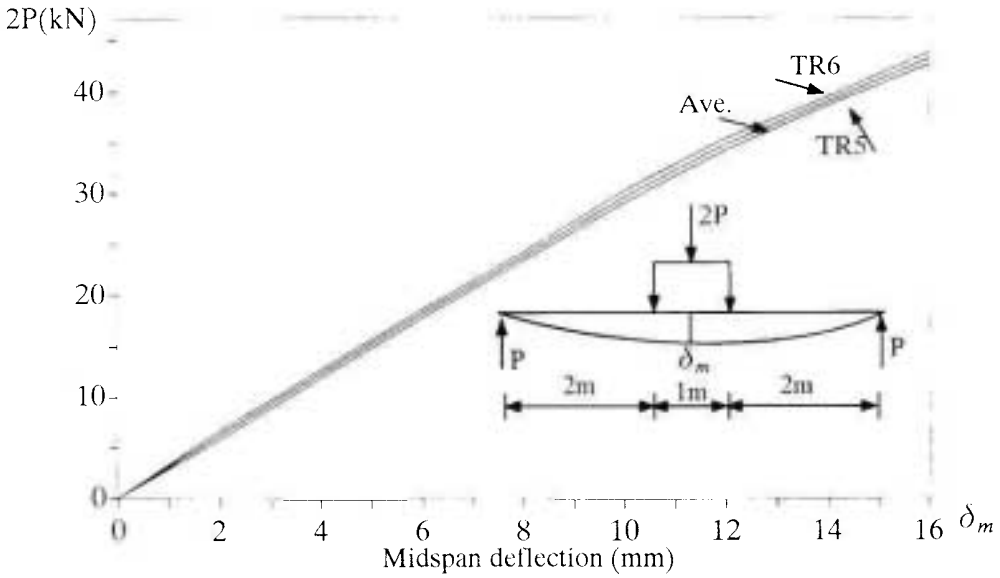

Figure 5. Load-deflection of profiled trough girder B2

response is initially linear, but the tangent stiffness is reduced in the postbuckled range as the loading is increased.

Local Buckling Loads

The local buckling load for each beam was determined in the experiments from the load-strain relationships measured in the compression zone of the trough girders. For beam B1 the load at which the load-strain relationship became non-linear was when the load from the jack $2P_{ol}$ was close to 20 kN where P_{ol} is local buckling load.

The local buckling load of the beam B2 was also obtaiend from the load-strain relationship, which became non-linear when the load in jack $2P_{ol}$ was about 35 kN. As noted in several experimental studies, including those undertaken by Rhodes and Harvey [11], the elastic local buckling load is often masked, and this is probably attributable to the presence of initial geometric imperfections [9].

Measured Buckling Half-wavelengths

The local buckling half-wavelenght of the two beams was measured using a ruler against the edge of each beam. It was observed that the beams B1 and B2 had a local buckling half-wavelength of 75*mm* and 60*mm*, respectively.

Postbuckled Bending Stiffness

The post-local buckling bending stiffness of the trough girders was determined from the moment-curvature response. The moment-curvature curves were most conveniently determined from the linear portion of the load-deflection reponse of the troughs and the load-strain response for the non-linear portion. The moment-curvature response for each beam at midspan is shown in Figure 6 for beams B1 and B2. The tangent to these curves represents the flexural rigidity. This property is initially constant, but reduces as the postbukling deformations become more severe. The relationship between the deflection as measured and the curvature was obtained for the constant moment region using the step function technique [12].

THEORETICAL COMPARISON

The initial buckling finite strip model developed by Azhari and Bradford [7] which uses bubble functions

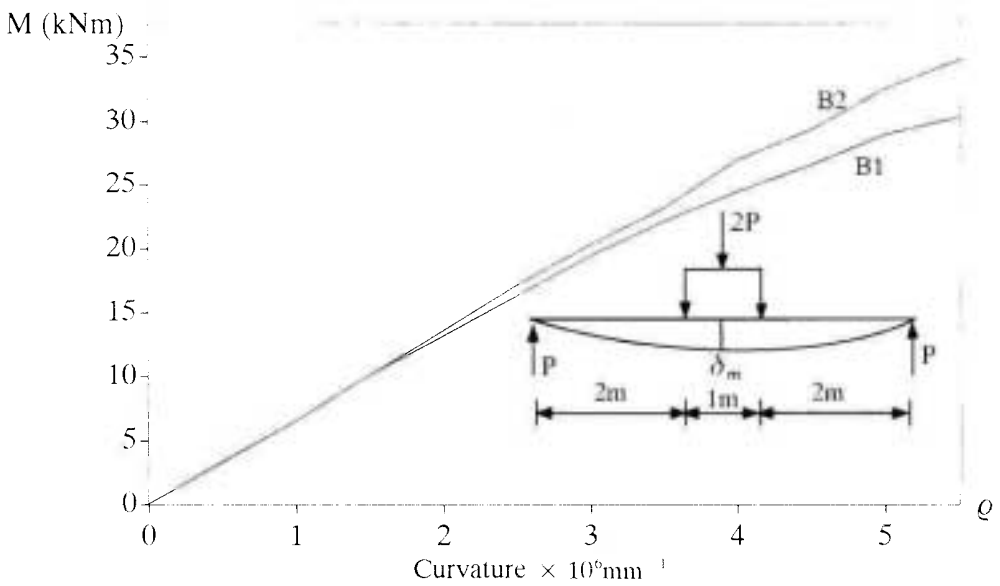

Figure 6. Moment-curvature response of profiled trough girders B1 and B2.

was utilized to calculate the initial local buckling stress and local buckling half-wavelength λ of the beams B1 and B2 which were tested. These compared exactly with the solution of Equation 14. Note that since the profiled trough girders were braced internally, top chord bracing might have influenced the stiffness and consequently the position of the neutral axis of the girders. An analysis was undertaken when the bracing was both present and absent, and the results were compared with those of the experiments.

Initial Local Buckling

The initial local buckling load was calculated from the finite strip analysis for the beams, for the cases with bracing included and excluded. The local buckling half-wavelength was varied and the local buckling stress was determined. The resutls of these studies are shown in Table 1. The theoretical results for the local buckling stress were then used to calculate the critical moment M_{ol} and the critical value of the load from the jack $2P_{ol}$. The following relationships were used and obtained from Figure 3,

$$P_{ol} = \frac{\sigma_{ol} I_{xx}}{1.925\,\bar{y}} \qquad (15)$$

The results in Table 1 shows that the local buckling analysis for beam B1 with the bracing absent compared more favorably than the analysis with bracing present. The local buckling stress σ_{ol} versus load buckling half-wavelength λ for these cases are shown in Figures 7 and 8 respectively. Thus it can be concluded that the internal bracing truss had little effect on the bending stiffness of the trough. The experimental results were also more accurately modelled from the theory for beam B2 without including the bracing. The theoretical local buckling plots of stress versus half-wavelength ofor the braced and unbraced cases for beam B2 are given in Figure 8.

Post-local Buckling

Once the initial elastic local buckling stress was calculated for both beams, the post-local buckling behavior was then obtained using the nonlinear buckling model developed by Azhari and Bradford [8] and outlined in theory section

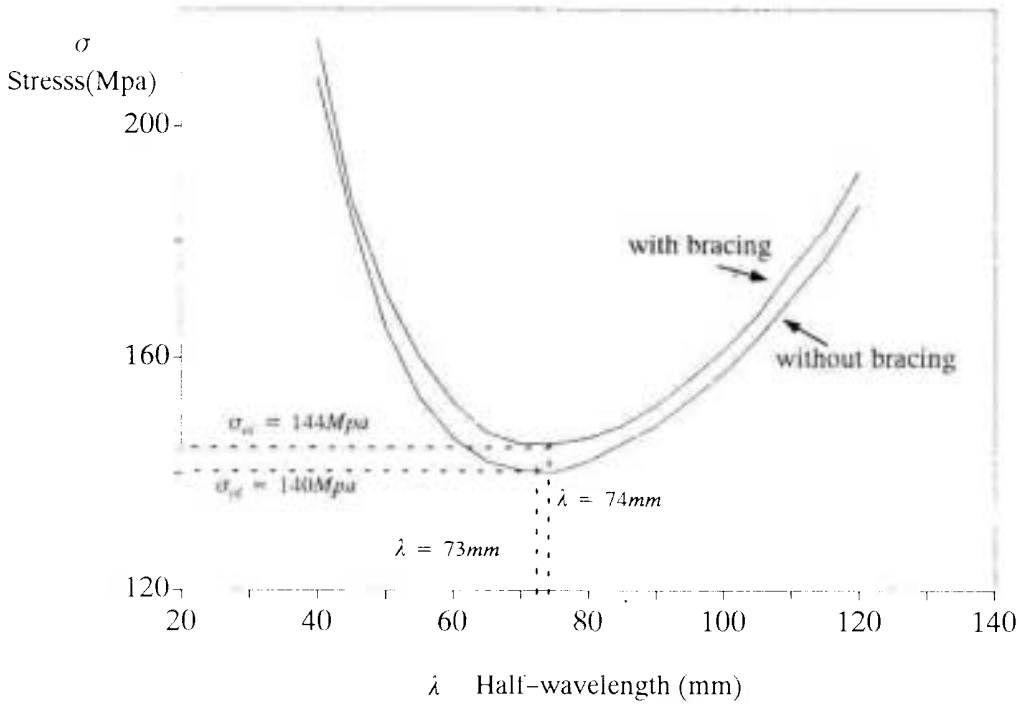

Figure 7. Stress versus local buckling half-wavelength for B1

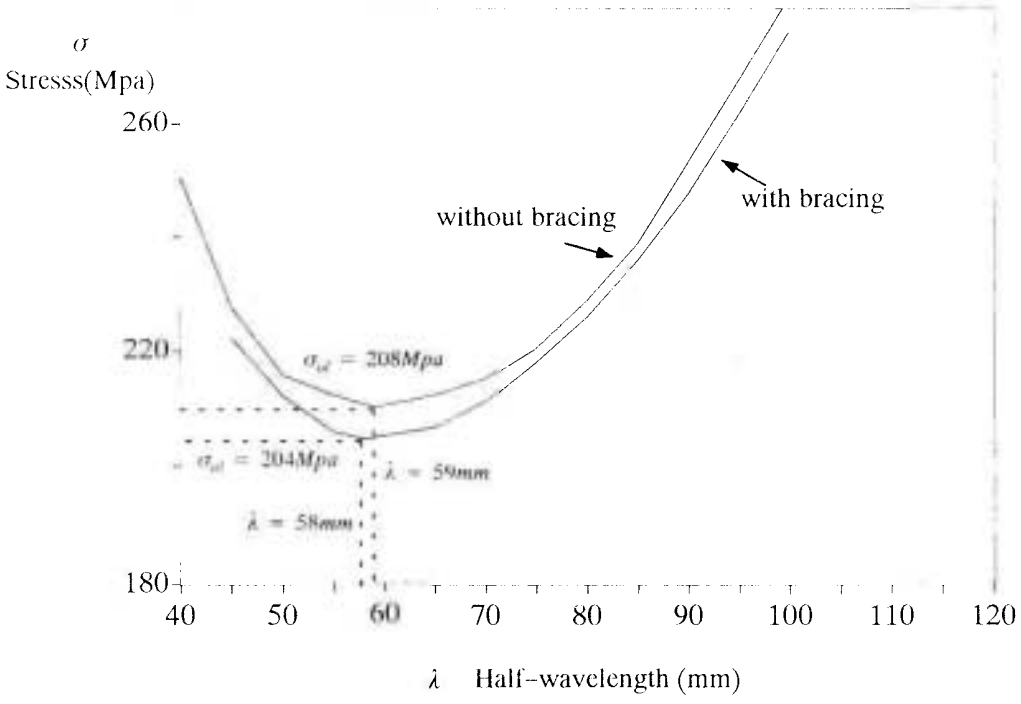

Figure 8. Stress versus local buckling half-wavelength for B2

TABLE 1. Local Buckling Stresses and Half-wavelengths.

Beam No.	Bracing	Theoretical local buckling stress σ_{ol} (MPa)	Theoretical local buckling half-wavelength λ (mm)	Theoretical local buckling load from jack $2P_{ol}$ (kN)	Experimental half wavelength λ (mm)	Experimental buckling locad $2P_{ol}$(kN)
B1	No	140	73	20.4	75	20
B1	Yes	144	74	31.9		
B2	No	204	58	34.6	60	35
B2	Yes	208	59	49.1		

The post-local buckling is able to predict the decrease in flexural stiffness of the member after local buckling has taken place. This analysis has been undertaken assuming both nongeometric imperfections and small geometric imperfection.

The post-local buckling behavior of trough girders B1 and B2 in pure bending was studied using the nonlinear finite strip method. Both perfect and imperfect sections were considered. The geometric imperfections $\{\Delta_0\}$ in the members were chosen to be the same as the buckling mode of each member alone as noted earlier, with a maximum value of 10% of the profile thickness, t.

For a given curvature, integration of the post-locally buckled stress distribution results in the development of an axial force. As the section is in pure bending, this axial force must vanish and so an additional uniform strain ε_0 was determined using a trial and error procedure at each value of the applied curvature.

At each value of curvature ρ, the moment was calculated by integrating the stress distribution over the area times its lever arm numerically. The effective flexural rigidity S^* was computed from the central slope of a quadratic fitted through three adjacent points on the moment-curvature curve derived in this way. Figure 9 shows the postbuckled stiffness ratio S^*/S for imperfect and perfect trough girder B1, while Figure 10 illustrates S^*/S for the trough girder B2, where S is the value of initial bending stiffness EI_{xx}.

Azhari and Bradford [8] showed that the minimum value of the post-locally buckled stiffness ratio S^*/S for an imperfect I-beam whose flange width and web depth are equal is close to 0.74. Figures 9 and 10 show that the minimum value of S^*/S is about 0.83 which is greater than the case of an I-beam. This is because in

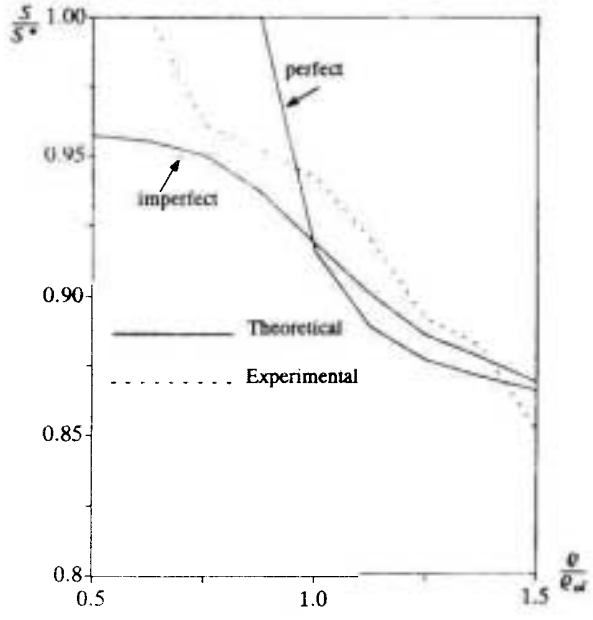

Figure 9. Postbuckled stiffness of perfect and imperfect trough girder B1.

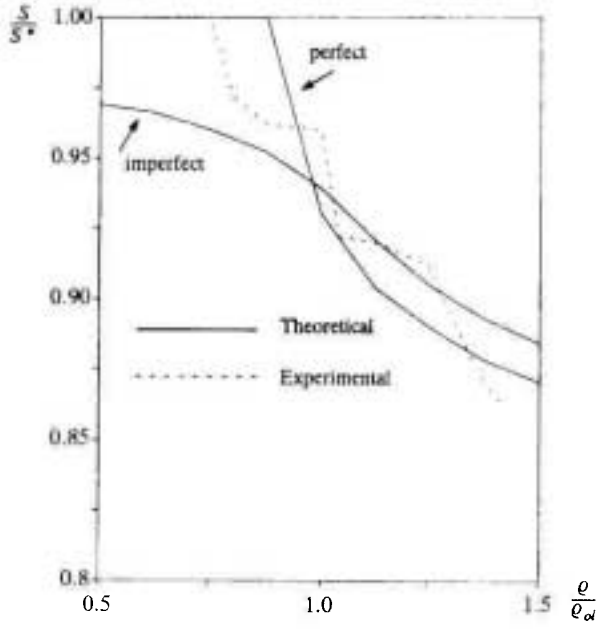

Figure 10. Postbuckled stiffness of perfect and imperfect trough girder B2.

the trough girders, only the top portion of the web is under severe local buckling and the reduction of stiffness in this portion does not affect the resultant moment greatly. However, in the I-beam the reduction in stiffness of the flange has a considerable effect on the resultant moment.

The bending stiffness ratio determined from the experiments using the moment-curvature relationship was then compared with that obtaiend from the theory using the post-local buckling solution. The results show that the post-local buckling stiffness with geometric imperfections predicted by the theory is conservative for the value of curvature less than about $1.25\rho_{ol}$; however for larger values of the curvature the prediction is unconservative. Figure 9 shows the experimental and theoretical values for the non-dimensional bending stiffness with the non-dimensional curvature for imperfections present and absent for the beam B1. Figure 10 illustrates the same relationships for the beam B2. The maximum imperfection of $0.1\,t$ selected for the analytical study is probably a little high, and the S^*/S curve calculated for an imperfection some where between $0.1t$ and perfect trough would match very well with the experiments. For the curvature above about, $1.25\rho_{ol}$, the post buckling half-wavelength changes, whilst the theoretical postbuckling model assumes that it is constant. The comparisons demonstrate the well-known fact that the postbuckling analysis is too stiff in the advanced stages of loading, although the disparity between the theory and the tests is not too severe.

CONCLUSION

The local buckling results of the experiments on empty profiled trough girders reported in this paper are in good agreement with the independent theoretical models with which they were compared. The results given are for re-entrant L rib type trough girders, and show good agreement for both initial and post-local buckling. Further research can be undertaken for trapezoidal and dove-tailed rib configurations which may also be deployed for profiled composite beams.

The results of the experiments have provided benchmark data for the hollow profiled trough girders used in profiled composite beam construction, by identifying the initial and post-local buckling behaviors of the trough system. The local and post-local buckling responses are particularly important for determining deflections of the troughs when supporting construction loads before the concrete is poured, so that the propping requirements can be assessed.

ACKNOWLEDGEMENT

This project was partially supported by Isfahan University of Technology. The experimental of this paper forms part of a programme into the strength and serviceability of steel-concrete members being undertaken at The University of New South Wales.

The authors would like to thank Dr. D. J. Oehlers and Dr. G. Sved for their helpful suggestions regarding the experiments.

REFERENCES

1. H. D. Wright, H. R. Evans and P. W. Harding, "The Use of Profiled Steel Sheeting in Floor Construction", *J. Const. Steel Research*, Vol. 7, No. 4, (1987), 279-295.
2. H. D. Wright, H. R. Evans and S. C. Gallocher, "Composite Walling", Proc. Int. Engg. Foundation. Conf. On Composite Construction, Potosi, Missori, USA, (1992)
3. D. J. Oehlers, "Composite Profiled Beams", *J. Struct. Engg. ASCE*, Vol. 119, No. 4, (1993), 1085-1100.
4. D. J. Oehlers, H.D. Wright and M. J. Burnet, "Flexural Strength of Profiled Beams", *J. Struct. Engg. ASCE*, Vol. 120. No. 2, (1994), 378-393.
5. B. Uy and M.A. Bradford, "Service Load Tests on Profiled Composite and Reinforced Concrete Beams", *Maga., Concrete Research*, Vol. 46, No. 166, (1994), 29-33.
6. N. S. Trahair and M. A. Bradford, "The Behavior and Design of Steel Structures," Chapman and Hall, 2nd edn., (1988).
7. M. Azhari and M.A. Bradford, "Local Buckling by the Complex Finite Strip Method Using Bubble Functions", *J. Engg. Mech., ASCE*, Vol. 120, No. 1, (1994), 43-57.
8. M. Azhari and M.A. Bradford, "The Use of Bubble Functions for the Post-local Buckling of Plate Assemblies by the Finite Strip Method", *Int. J. Num. Meth. Engg.*, Vol. 38, (1995), 955-968.
9. M. A. Bradford and G. J. Hancock, "Elastic Interaction of Local and Lateral Buckling in Beams", *Thin-Walled Struct.*, Vol. 2, (1984), 1-25.
10 R. H. Gallagher, S. Lien and S.T. Mau, "A Procedure for Finite Element Plate and Shell Pre and Postbuckling Analysis", Proc. Int. Conf. on Matrix Method of Structural Analysis, Wright-Patterson Air Force Base, Ohio, U.S.A., (1971), 857-879.
11. J. R. Rhodes and J. M. Harvey, "Plain Channel Section Struts in Compression and Bending Beyond the Local Buckling Load", *Int. J. Mecha. Scien.*, Vol. 8, (1976). 511-519
12. A. S. Hall, "An Introduction to the Mechanics of Solids," John Wiley and Sons, Sydney, (1988).